

Surface and Interface Analysis of Organic Electroluminescent Devices

Atsushi Murase, Takuya Mitsuoka, Noritake Isomura

有機EL素子の表面・界面の分析技術

村瀬篤，光岡拓哉，磯村典武

Abstract

The chemical and morphological structures of the surface and interface of organic electroluminescent devices were evaluated using surface analysis techniques. The effect of surface polarity of the substrate with regard to the morphology of an overlying hole-transport material was investigated by atomic force microscopy, decomposition of the light-emitting material during depositing cathode material was

investigated by x-ray photoelectron spectroscopy and time-of-flight secondary ion mass spectrometry, and the growth mechanism of dark spots in devices was investigated based on the mass spectrometry results. It was confirmed that these analytical methods are useful for solving problems related to the development of EL devices.

Keywords

Electroluminescent device, Atomic force microscopy, X-ray photoelectron microscopy, Time-of-flight secondary ion mass spectrometry, Interface, Dark spot

要 旨

有機EL素子における表面・界面の化学構造または形態を、種々の表面分析技術により評価を試みた。正孔輸送層の形態に及ぼす基板の極性の影響を原子間力顕微鏡 (AFM) により、発光層と陰極との界面における発光材料の化学構造をX線光電子分光 (XPS) と飛行時間型二次イオン質量分

析 (TOF-SIMS) により、素子の駆動により生成するダークスポットの生成メカニズムをTOF-SIMSによりそれぞれ調べた。その結果、これらの分析技術が素子の開発の各段階における諸問題の解決に有効であることが確認できた。

キーワード

EL素子，原子間力顕微鏡 (AFM)，X線光電子分光 (XPS)，飛行時間型二次イオン質量分析 (TOF-SIMS)，界面，ダークスポット

1. Introduction

Organic electroluminescent (EL) devices are expected to be used in various fields, offering excellent luminescence properties, if reliability long-life operation can be guaranteed.¹⁾ In order to improve the reliability of EL devices, it is necessary to evaluate the structure of the constituent organic materials and the degradation mechanisms at the surfaces and interfaces. The authors have attempted to evaluate the chemical or morphological structures by various surface analysis techniques.^{2, 3)} This paper describes the morphological characterization of a hole transporting material on a substrate by atomic force microscopy (AFM), the evaluation of degradation of an emitting material at the interface during cathode deposition by x-ray photoelectron spectroscopy (XPS) and time-of-flight secondary ion mass spectrometry (TOF-SIMS), and the analysis of dark spots in EL devices by TOF-SIMS. These analyses were confirmed to be useful to solve problems related to each of the processes involved in the development of these devices.

2. Experimental

2.1 Materials

The structure of the EL device examined in this study is shown in **Fig. 1**. The EL device had a typical two-organic layer structure of indium-tin-oxide (ITO) as a transparent anode, triphenylamine-

tetramer (TPTE) as a hole transporting layer, tris (8-hydroxyquinoline) aluminum (Alq₃) as an emitting layer, and Mg-Ag or Al as the metal cathode. The chemical structure of TPTE and Alq₃ are shown in **Fig. 2**. The total thickness of the device was ~400 nm. The device was covered with an MgF₂ thin film protector of ~300 nm in thickness. All materials are commercially available reagents. TPTE and Alq₃ were refined by vapor deposition before use.

2.2 Sample preparation

2.2.1 Hole transporting layer on Si substrate

An H-terminated hydrophobic Si (100) surface was prepared by dipping in 0.5% HF for 5 min. The hydrophilic surface was prepared from the hydrophobic surface by dipping in H₂SO₄/H₂O₂ (4/1) for 5 min and rinsing with ion-exchanged water.⁴⁾ TPTE films were deposited on the hydrophobic or hydrophilic surface by evaporation.

2.2.2 Al/Alq₃ interface

The layer structure of Al/Alq₃ was prepared on a Si substrate by vacuum evaporation. The Alq₃ film, 60 nm in thickness, was thermally evaporated in a vacuum of 1×10^{-7} Torr. Alq₃ films were then transferred to the connected ultrahigh-vacuum preparation and analysis chambers via the mobile chamber under 1 atm of N₂. XPS and TOF-SIMS spectra were measured immediately after the deposition of the Al film under a vacuum of 1×10^{-7} Torr (deposition rate of 0.5 nm/s). The thickness

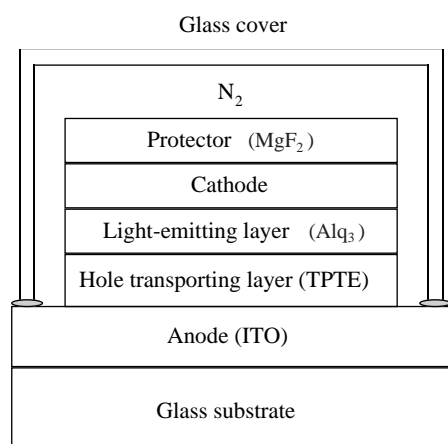


Fig. 1 Schematic illustration of the structure of the studied EL device.

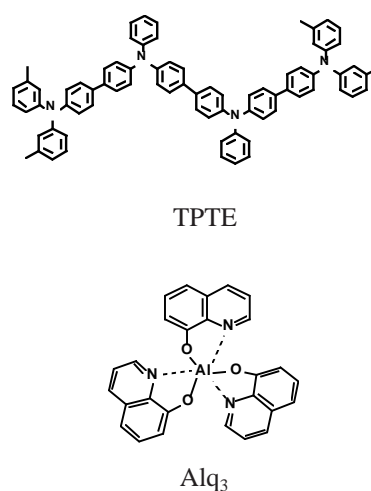


Fig. 2 Chemical structures of triphenylamine-tetramer (TPTE) and tris (8-hydroxyquinoline) aluminum (Alq₃).

was monitored by a quartz thickness monitor. The Al film was 0.5 nm thick.

2.2.3 Dark spot formation in EL devices

The formation of dark spots was induced by exposing the surface of the ITO to the ambient atmosphere for 2 days prior to vapor deposition of the organic layers, cathode, and MgF_2 protector. A large number of dark spots of approximately 50-100 μm in diameter grew due to exposure. An optical micrograph of the dark spots is shown in **Fig. 3**. The occurrence and growth of dark spots were observed by a video microscope system. Based on the previous paper, it was predicted that the dark spots grew at the interface between the cathode and the Alq_3 layer of the EL device.¹⁾ Therefore, chemical structural analysis of the dark spots was performed by TOF-SIMS analysis of the tape stripped surfaces.

2.3 Analysis

2.3.1 AFM

Tapping-mode AFM measurements were carried out using a Digital Instruments Nanoscope IIIa and D3100 AFM in air at room temperature, with a single-crystal Si cantilever with a tip radius of 5-20 nm. The spring constant of this cantilever typically used for tapping-mode experiments in air was 260-410 N/m, and the scan frequency was about 1.0 kHz. Tapping mode is effective for examining the surface morphology on very soft surfaces like living cells.

2.3.2 TOF-SIMS

TOF-SIMS measurements were performed using a Physical Electronics TFS-2100 (TRIFT 2) instrument controlled by Cadence software. High-

mass resolution spectra of $M/\Delta M > 3000$ at m/z 27 (Al^+) or 25 (C_2H^+) were acquired using a bunched $^{69}\text{Ga}^+$ ion pulse at an impact energy of 15 keV, an ion current of 600 pA per pulse, a pulse width of 14 ns (700 ps after bunching), and a pulse frequency of 10 kHz. High lateral resolution (0.2 μm) images and low mass resolution ($M/\Delta M > 300$) spectra were acquired using an unbunched $^{69}\text{Ga}^+$ ion pulse at an impact energy of 25 keV, an ion current of 600 pA for 1 pulse, a pulse width of 30 ns, and a pulse frequency of 10 kHz. Total ion doses in these measurements were approximately $< 1 \times 10^{12}$ ions/ cm^2 . Spectra from the regions of interest in a secondary ion image were acquired using the Cadence software. In all cases, two different positions of the same surfaces were measured in order to estimate the reproducibility of the TOF-SIMS data.

2.3.3 XPS

XPS measurements were performed using a Physical Electronics PHI-5500MC with a monochromatic $\text{AlK}\alpha$ x-ray source (1486.6 eV) in an ultrahigh vacuum. Spectra were recorded at 23.5 eV pass energy, 150 W x-ray source power, and a take-off angle of 70° .

3. Results and discussion

3.1 Morphology of TPTE layer on Si substrate

The effect of surface polarity of the substrate on the morphology of the TPTE layer was investigated by AFM. **Figure 4** shows an AFM image of a TPTE layer on Si substrate. The surface of the Si substrate

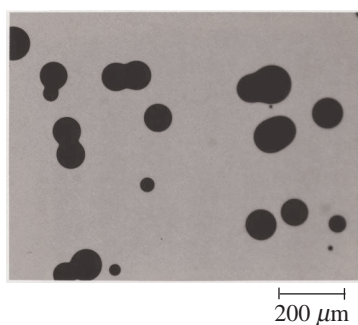


Fig. 3 Optical micrograph of dark spots grown in the device.

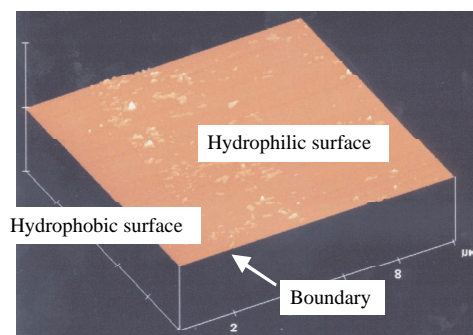


Fig. 4 AFM image of the surface of TPTE layer deposited on the hydrophilic and the hydrophobic surfaces of Si wafer.

is half hydrophilic, half hydrophobic. From the AFM image, it was found that the morphology of TPTE layer is flat on hydrophobic surface, and rough on hydrophilic surface. As TPTE is non-polar, the above results mean that non-polar molecules wet a hydrophobic surface and are repelled from a hydrophilic surface. It can be concluded that the morphology of the organic layers is affected by the surface polarity of the substrate. This phenomenon was not observed in SEM images. Therefore, AFM is expected to be a useful tool for evaluation of the morphology of organic thin layer such as organic EL devices.

3. 2 Decomposition of Alq₃ during cathode deposition

Figure 5 shows the core-level peaks of N_{1s}, O_{1s} and C_{1s} in the XPS spectra measured immediately after the deposition of Al on Alq₃ in the Al/Alq₃ systems. The peaks of N_{1s}, O_{1s} and C_{1s} from Alq₃ are shown as references. The N_{1s} peak from Alq₃ was observed at 400.3 eV, and that from Al/Alq₃ was composed of two overlapping peaks at 400.3 eV and

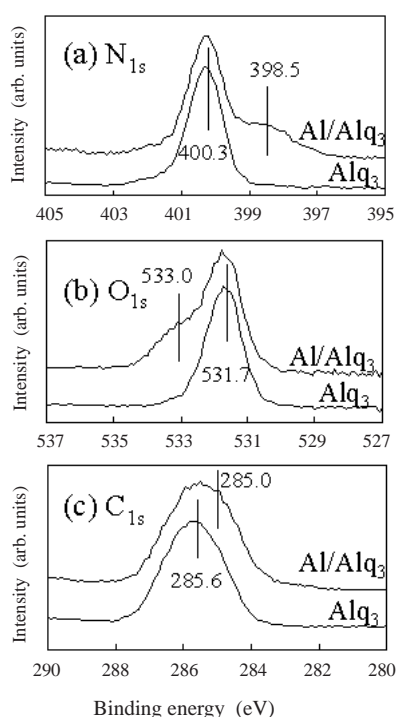


Fig. 5 XPS spectra measured immediately after deposition of each layer in Al/Alq₃.
(a) N_{1s} (b) O_{1s} (c) C_{1s}

398.5 eV. The N_{1s} peak at 398.5 eV is in close agreement with that reported for quinoline⁵⁾ in the sense that the positions of the peaks are lower than that of the Alq₃ peak, which suggests the decomposition of Alq₃. On the other hand, the O_{1s} peak from Alq₃ was observed at 531.7 eV, and that from Al/Alq₃ was composed of two overlapping peaks at 531.7 eV and 533.0 eV. Similarly, as shown in Fig. 5(c), the C_{1s} peak from Alq₃ was observed at 285.6 eV, and that from Al/Alq₃ was composed of two overlapping peaks at 285.6 eV and at about 285.0 eV. If the cleavage occurs at the C-O bonds of Alq₃, it is expected that the binding energy of carbon would decrease and that the binding energy of oxygen would increase by electron transfer from oxygen back to carbon. This assumption is in good agreement with the changes in the spectra of O_{1s} and C_{1s}, and supports the idea of decomposition of Alq₃ suggested by the change in the spectra of N_{1s}. Therefore, it is possible to conclude that the deposition of Al on Alq₃ causes the decomposition

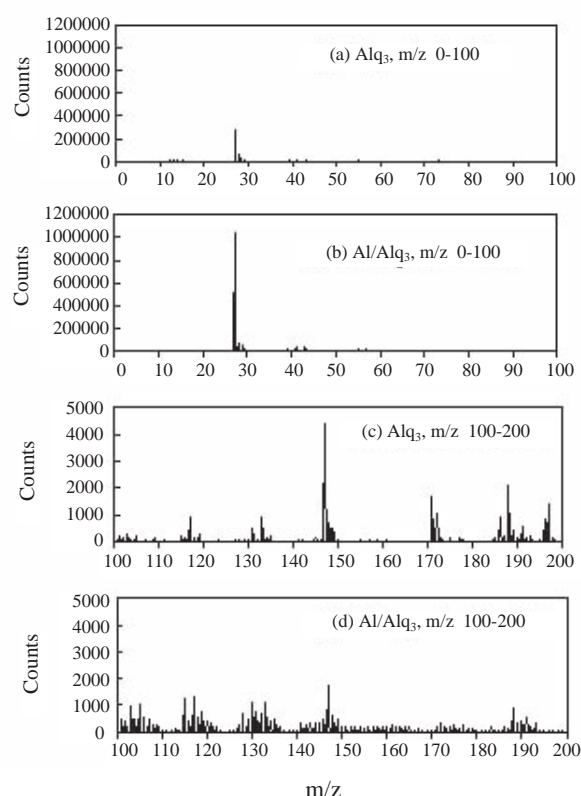


Fig. 6 Positive ion spectra of the surfaces of Alq₃ and Al/Alq₃.

of Alq_3 .

Figure 6 shows the positive ion TOF-SIMS spectra of Alq_3 and Al/Alq_3 in representative regions. The intensities of the peaks at m/z 27, 103, 105, 115, 128, and 130 increased after Al deposition on Alq_3 , and were assigned to Al^+ , C_8H_7^+ , C_8H_9^+ , C_9H_7^+ , NC_9H_6^+ , and $\text{C}_9\text{H}_7\text{N}-\text{H}^+$, respectively. The peak at m/z 130 was considered to correspond to the secondary ion from quinoline. It is possible that the origin of the molecules exhibiting peaks at m/z 103, 105, 115, and 128 was quinoline. This finding suggests that Alq_3 is decomposed into quinoline by the deposition of Al on Alq_3 .

3.3 Analysis of dark spots by TOF-SIMS

3.3.1 Determination of the position of a tape-stripped surface

The cathode side of the devices was peeled off with adhesive tape from the anode side. To determine the position of the surface mechanically stripped with adhesive tape, TOF-SIMS spectra were obtained from both sides of the stripped interface. **Figure 7** shows the positive spectra of the tape-stripped surfaces of an undegraded device. In the spectrum of the cathode side, Mg^+ originating from the constituent element of the cathode was the main detected component, and the fragment ions originating from Alq_3 such as Al^+ and Alq_2^+ could be

clearly seen. In the spectrum of the anode side, fragment ions originating from Alq_3 were the main detected component, with small signals due to Mg^+ . These results indicate that the tape-stripping exposed the interface of the cathode and the Alq_3 layer of the EL device.

In the spectra of Fig. 7, $\text{C}_9\text{H}_8\text{N}^+$ at m/z 130 originating from quinoline, which indicates the decomposition of Alq_3 , was clearly detected on the cathode side but not on the anode side. As described in the previous section, vapor deposition of cathode material onto the Alq_3 layer causes decomposition of Alq_3 and generates quinoline at the interface. Therefore, the fragment ions of Alq_3 detected on the cathode side are assumed include both Alq_3 , transferred from the light-emitting layer, and decomposed Alq_3 generated upon vapor deposition of the cathode and which remained on the cathode side after tape-stripping. Neither ITO nor TPTE were detected on either the cathode or anode side. This result indicates that tape-stripping did not damage the specimen between the light-emitting layer and the anode.

3.3.2 Secondary ion imaging of dark spots

Secondary ion images obtained by TOF-SIMS analysis of the cathode and anode sides of the tape-stripped surfaces are shown in **Figs. 8** and **9**,

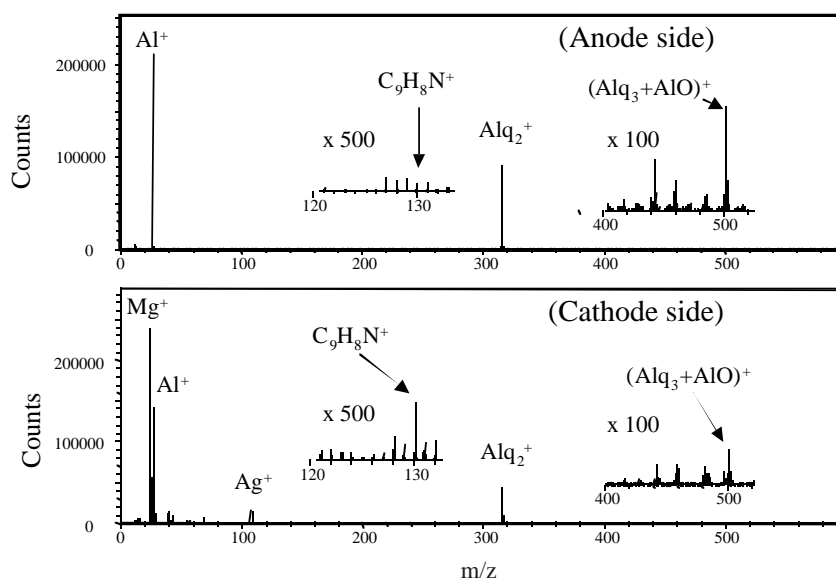


Fig. 7 Positive ion spectra of tape-stripped surfaces of an undegraded device.

respectively. The measured positions of the positive and negative ion images are not the same. As mentioned in the last section, the main positive ions on the cathode side were Mg^+ originating from cathode material, and those on the anode side were Al^+ and Alq_2^+ originating from Alq_3 . Therefore, the interface between the cathode and the Alq_3 -emitting layer was exposed by tape-stripping. On some of

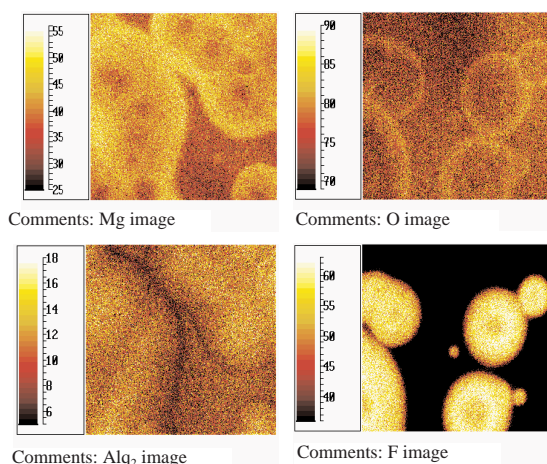


Fig. 8 Secondary ion images obtained by TOF-SIMS analysis of the cathode side of the tape-stripped surfaces of the EL device. The field of view is $100 \times 100 \mu\text{m}$.

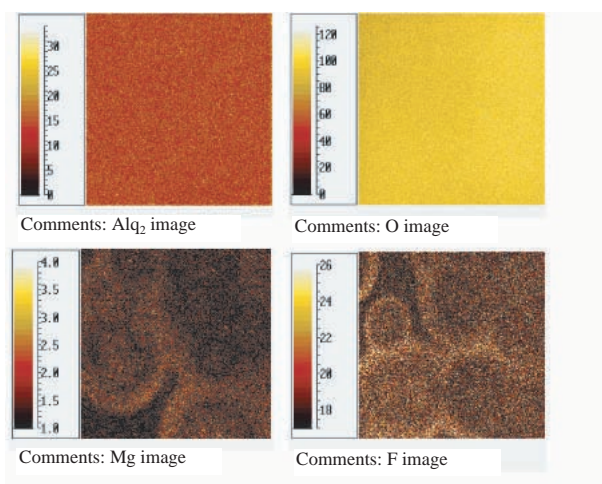


Fig. 9 Secondary ion images obtained by TOF-SIMS analysis of the anode side of the tape-stripped surfaces of the EL device. The field of view is $100 \times 100 \mu\text{m}$.

the secondary ion images at the tape-stripped surfaces, many circles corresponding to dark spots were observed.

Cathode side of the tape-stripped surface: As shown in Fig. 8, many circles about $20\text{--}50 \mu\text{m}$ in diameter were observed in secondary ion images of Alq_2^+ , Mg^+ , O^- , and F^- . Among them, Alq_2^+ and Mg^+ originate from the Alq_3 -emitting material and the cathode material, respectively. In the Alq_2^+ image, the ion intensity was highest near the center of the circles. In the Mg^+ image, in reverse, the ion intensity was largest near the circumference and relatively small near the center of the circles. This result suggests that the Alq_2^+ on the inside of the circles did not react with Mg but was transferred from the Alq_3 layer by tape-stripping. The distribution of O^- , on the other hand, was partly similar to that of Mg^+ at the point where the ion intensity was highest near the circumference of the circles. This result suggests that the distribution of Mg^+ partly originates from oxidized Mg. It is assumed that the yield of Mg^+ was enhanced by combination with oxygen because the ionization yields of metal elements are known to be enhanced by combining with electronegative elements such as oxygen.⁶⁾ The distribution of F^- was also partly similar to that of Mg^+ at the point where the ion intensity was relatively low near the center of the circles. Therefore, part of the Mg^+ image was estimated to originate from fluorinated Mg, and it is assumed that the yield of Mg^+ was enhanced by combination with fluorine as with oxygen. F^- is estimated to originate from the MgF_2 protector, but it is not clear whether the F^- image in Fig. 8 is the image of the MgF_2 protector itself or of the fluorinated cathode material. From these images, therefore, it is concluded that, on the inside of the dark spots, the cathode material was oxidized or fluorinated and part of the light-emitting layer was transferred onto the cathode side by tape-stripping.

Anode side of the tape-stripped surface: As shown in Fig. 9, a large number of circles of Mg^+ and F^- corresponding to dark spots were also observed on the cathode side. They are considered to originate from MgF_2 , which was used for the protector, because of the similar distributions except at the point where a small nucleus under $1 \mu\text{m}$ in diameter

was observed in the Mg^+ image in the center of the circles. This image of MgF_2 indicates a remaining trace of invasion from the cathode side of the device. MgF_2 is not able to flow by itself because it is solid under ambient conditions. It is possible that a liquid dissolved MgF_2 and carried it into the interface. Because of the high solubility of MgF_2 in water, it is expected that MgF_2 can be carried by moisture in this way. Therefore, it is proposed that an invasion of moisture from the cathode side of the device into the cathode/ Alq_3 interface caused oxidation of the constituent element Mg of the cathode, forming a dark spot. In the Alq_2^+ image of the anode side, on the other hand, no circle was observed as shown in Fig. 9. This result indicates that the growth of dark spots was caused by changes only at the cathode/ Alq_3 layer interface, with no chemical or structural changes in the overall Alq_3 layer.

3.3.3 Secondary ion spectra of a dark spot

The distribution of Alq_2^+ and Mg^+ (Fig. 8) suggested that the Alq_3 component is transferred from the inside of a dark spot by tape-stripping. To evaluate the transferred component in more detail, the fragment pattern of Alq_3 on the inside of a dark spot was compared with that on the outside. Positive secondary ion spectra of the inside and the

outside of a dark spot, obtained by TOF-SIMS analysis of the region of interest on the cathode side are shown in Fig. 10. From these spectra, $\text{C}_9\text{H}_8\text{N}^+$ at m/z 130 originating from quinoline, which indicates the decomposition of Alq_3 , was detected on the outside of the dark spot clearer than on the inside, and the intensity ratios of the fragment ions of Alq_3 such as Al^+ , Alq_2^+ , and $(\text{Alq}_3 + \text{AlO})^+$ are different in each spectrum. The ratios of $\text{Alq}_2^+/\text{Al}^+$ and $(\text{Alq}_3 + \text{AlO})^+/\text{Alq}_2^+$ on the inside are larger than those on the outside. This tendency is similar to the relation between the cathode side and the anode side of an undegraded device (Fig. 7). On the basis of these results, it is concluded that undecomposed Alq_3 adsorbed onto the cathode surface on the inside of a dark spot and remained at the cathode side of the tape-stripped surface.

Liew et al. concluded that the growth of dark spots occurs primarily due to cathode delamination, based on the fact that the Alq_3 at the sites of the dark spots is still functional.⁷⁾ However, from our results, it is suggested that on the inside of the dark spots, the affinity of the cathode material and Alq_3 was stronger than on the outside of the dark spots, and it is assumed that delamination of the cathode/ Alq_3 layer interface does not occur easily. When the

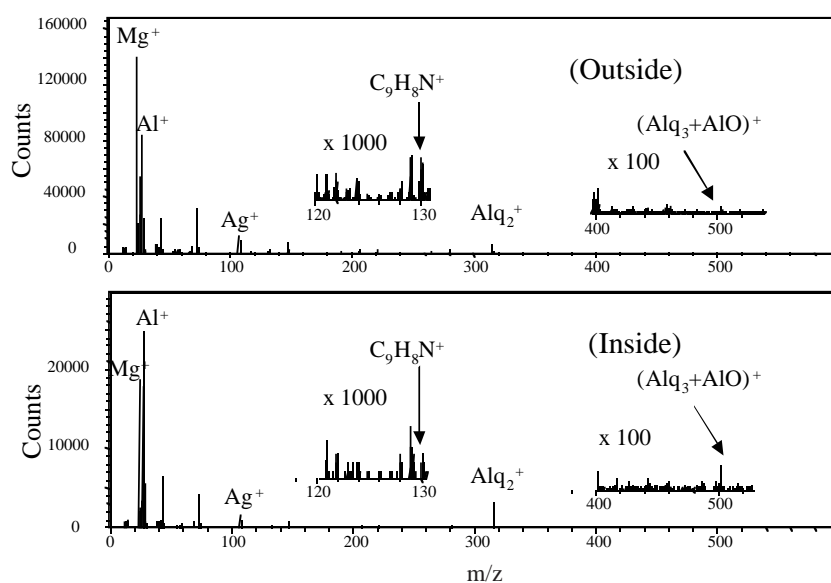


Fig. 10 Positive ion spectra of the inside and the outside of a dark spot obtained by the TOF-SIMS analysis of the cathode side using an ROI function.

cathode was peeled off, part of the Alq₃ at the interface may be removed with the cathode, and the remaining Alq₃ would still function as a light-emitting layer. Also in our results, there were few images of dark spots on the anode side after tape-stripping.

4. Conclusions

(1) From AFM image of TPTE on a Si substrate, it was found that the morphology of TPTE layer was affected by the polarity of the substrate.

(2) From the results of XPS and TOF-SIMS analyses of the Alq₃ surface with one monolayer deposition of Al, it was found that Alq₃ is decomposed into quinoline by the deposited Al.

(3) From the results of TOF-SIMS analysis of a tape-stripped surface of EL devices, it was found that an invasion of moisture from the cathode side of the device into the cathode/Alq₃ interface caused oxidation of the constituent element Mg of the cathode, forming a dark spot.

(4) From the results described above, it was confirmed that surface analysis techniques such as AFM, XPS, and TOF-SIMS are useful for solving problems related to the development of organic EL devices.

Acknowledgments

This study was supported by the members of the EL project of Toyota Central R&D Labs., Inc.

References

- 1) Carver, G. E. and Velasco, V. J. : "Optical Testing Methods for Organic Electroluminescent Displays", *Synthetic Metals*, **91**(1997), 117
- 2) Isomura, N., Mitsuoka, T., Ohwaki, T. and Taga, Y. : "Chemical Structure of Aluminum/8-Hydroxyquinoline Aluminum Interface", *Jpn. J. Appl. Phys.*, **39**(2000), 312
- 3) Murase, A., Ishii, M., Tokito, S. and Taga Y. : "Analysis of Dark Spots Growing in Organic EL Devices by Time-of-Flight Secondary Ion Mass Spectrometry", *Anal. Chem.*, **73**(2001), 2245
- 4) Miki, K., Sakamoto, K. and Sakamoto, T. : "Surface Preparation of Si Substrates for Epitaxial Growth", *Surf. Sci.*, **406**(1998), 312
- 5) Xie, X. and Oelhafen, P. : "Electronic Structure of Plasma Polymers of Quinoline", *Thin Solid Films*, **278**(1996), 118

- 6) Stormes, H. A., Brown, K. F. and Stein, J. D. : "Evaluation of a Cesium Positive Ion Source for Secondary Ion Mass Spectrometry", *Anal. Chem.*, **49**(1977), 2023
- 7) Liew, Y. -F., Aziz, H., Hu, N. -X., Chan, H. S. -O., Xu, G. and Popovic, Z. : "Investigation of the Sites of Dark Spots in Organic Light-emitting Devices", *Appl. Phys. Lett.*, **77**(2000), 2650

(Report received on Oct. 9, 2002)



Atsushi Murase 村瀬篤

Year of birth : 1955

Division : Materials Analysis Lab.

Research fields : Surface and microanal. of organic mater., Appl. of time-of-flight secondary ion mass spectrometry (TOF-SIMS), Anal. of polym. degradation

Academic degree : Dr. Eng.

Academic society : Jpn. Soc. Anal. Chem., Soc. Polym. Sci., Jpn. Soc. Automot. Eng. Jpn., Mater. Life Soc.

Awards : Award of Tokai Chem. Ind., 1997.

R&D 100 Award, 1999.

Technical Award, Jpn. Soc. Anal. Chem., 2000.



Takuya Mitsuoka 光岡拓哉

Year of birth : 1966

Division : Materials Analysis Lab.

Research fields : Dev. of Chem. Force Microscopy, Dev. of Organic Transistor, Appl. of Scanning Probe Microscopy

Academic society : Jpn. Soc. Anal. Chem., Soc. Polym. Sci., Jpn.

Awards : Award of Tokai Chem. Ind., 1999.



Noritake Isomura 磯村典武

Year of birth : 1968

Division : Materials Analysis Lab.

Research fields : Microbeam anal., Surface and interface anal. by photoemission spectroscopy and scanning probe microscopy, Interface anal. for organic electroluminescent device

Academic society : Jpn. Soc. Appl. Phys.